Nonequilibrium phase transition in the electronic transport of *p*-type germanium at low temperatures

M. Lehr, R. P. Huebener, U. Rau, J. Parisi, W. Clauss, J. Peinke, and B. Röhricht
Physikalisches Institut, Lehrstuhl Experimentalphysik II, Universität Tübingen, D-7400 Tübingen, West Germany

(Received 27 February 1990; revised manuscript received 9 July 1990)

We investigate low-temperature impact-ionization breakdown of extrinsic germanium with the help of both time-averaged and time-resolved current-voltage measurements. Under variation of the lattice temperature as an appropriate thermodynamic control parameter, the underlying nonlinear physics displays a second-order nonequilibrium phase transition. The characteristic critical exponents evaluated reveal a scaling behavior consistent with the predictions of the Landau theory. Finally, an analogy to the well-known van der Waals gas equilibrium system is elucidated.

I. INTRODUCTION

In the temperature range of liquid helium and in the limit of very small applied electric fields, an extrinsic semiconductor shows a high electric resistivity, since almost all charge carriers are frozen out at the impurities. If the electric field is increased, the few charge carriers not bound to the impurities are accelerated, and at a critical field strength their energy becomes sufficiently high (hot electrons) for generating additional free carriers by means of the impurity impact-ionization process. The autocatalytic nature of this carrier multiplication process results in strongly nonlinear electronic transport behavior and, in particular, in the development of temporal and spatial structures in the electric resistivity of the semiconductor crystal.[1-3] Apparently, during avalanche breakdown at sufficiently low temperatures, a spatially and/or temporally homogeneous conducting state becomes unstable, and a more complex nonequilibrium state becomes more favorable. Some of the simplest and most observed spatial structures generated during semiconductor avalanche breakdown at low temperatures are current filaments, i.e., channels of high local electric conductivity arranged parallel to the electric-field direction and embedded within an environment with much lower conductivity. Recently, this current filamentation has been imaged with high spatial resolution by means of low-temperature scanning electron microscopy (LTSEM). The latter experiments were performed with *p*-type Ge[1,4,5] and *n*-type GaAs.[6] In particular, the experiments with *n*-type GaAs (Ref. 6) have clearly demonstrated the close correlation between the detailed structure of the current-voltage (*I-V*) characteristics and the nucleation and growth process of the individual current filaments.

An important question concerns the variation of the spatiotemporal structures generated during low-temperature electronic breakdown with the thermodynamic control parameters such as the lattice temperature. Here relevant information can be expected to be obtained from measurements of the *I-V* characteristics, since the connection between the spatiotemporal structures and the latter has been established experimentally, at least in the case of current filaments.[1,4-6] Indeed, recent studies in *p*-type Ge have revealed a strong qualitative change of the *I-V* characteristics with increasing temperature.[7] These experiments have suggested that in the *p*-type Ge samples investigated current filamentation exists only in a narrow temperature range of a few K above 4.2 K. Furthermore, the disappearance of the filamentary structure with increasing temperature appeared to display distinct features of a nonequilibrium phase transition. According to these results, low-temperature electronic breakdown in semiconductors represents a fruitful object for studying principles of the development of spatiotemporal dissipative structures, and further detailed measurements look highly promising.

In this paper, we report on measurements of the *I-V* characteristics in *p*-type Ge samples performed in the temperature range between 4 and 10 K. In this temperature range a qualitative change of the *I-V* characteristic from *S*-shaped to monotonic behavior is observed with increasing temperature. Expanding the voltage as a power series in the current, critical exponents can be defined analogous to the Landau theory of equilibrium phase transitions. The values of the critical exponents we have obtained are consistent with the predictions of the Landau theory. A more detailed report on our investigations has been given elsewhere.[8]

II. EXPERIMENTAL PROCEDURES

The sample material was single-crystalline *p*-doped germanium with an In acceptor concentration of about 3×10^{14} cm^{-3} and a room-temperature resistivity of 10 Ω cm. The sample crystals were about 3 mm wide and 10 mm long. The results reported in the following were obtained for two samples with a thickness of 200 (sample 1) and 260 μm (sample 2), respectively. Ohmic contacts of rectangular shape were fabricated on one of the two largest specimen surfaces by vacuum deposition of Al and standard photolithography. For sample 1 the contacts were 2.0 mm wide, and the distance between the contacts was 2.0 mm. For sample 2 the corresponding dimensions were 3.0 and 3.44 mm, respectively.

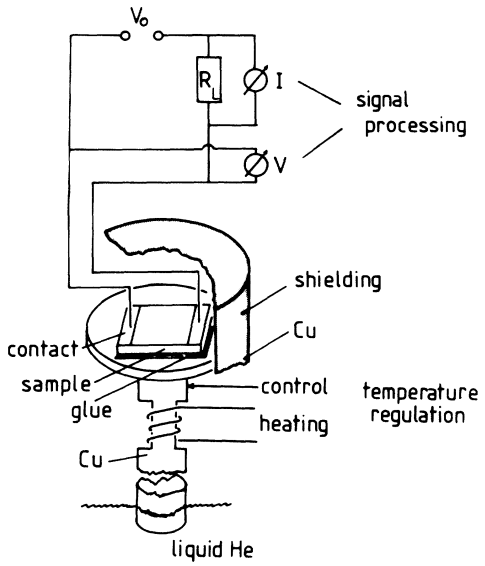

FIG. 1. Schematics of the sample configuration and the electronic measuring circuit.

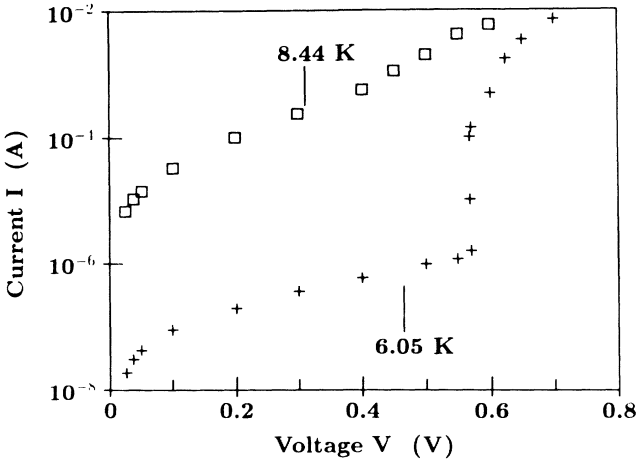

FIG. 2. Logarithm of the current vs the voltage along the sample for 6.05 and 8.44 K. Sample 2.

For the low-temperature experiments the samples were mounted in a copper can partly immersed in liquid He. The sample crystal was glued to a sapphire disk using Stycast cement, whereas the sapphire disk was clamped with good thermal contact to a copper block, the temperature of which could be controlled by means of a heater and a temperature sensor. In this way, the sample temperature could be regulated with an accuracy of about 5 mK in the range between 1.7 and 20 K.

The essential part of the sample configuration and the electronic measuring circuit is shown schematically in Fig. 1. The series connection of sample and load resistor R_L is attached to the voltage source. The lead wires connected to the sample and the load resistor served to measure the voltage drop along the sample and the current, respectively. The value of R_L was varied in the range 10 Ω–20 MΩ, thereby allowing to approach closely the case of current-biased or voltage-biased operation.

III. CURRENT-VOLTAGE CHARACTERISTICS

In Fig. 2 we show a typical plot of the logarithm of the current versus the voltage drop along the sample for the two temperatures 6.05 and 8.44 K. At small voltages, below about 10 mV, the I-V characteristics display ohmic behavior in the form of straight lines passing through the origin (not shown in Fig. 2). In this voltage regime the current is carried only by thermally activated charge carriers. Here an analysis of the temperature dependence of the conductivity yields the activation energy $E_A = 12.3$ meV for the In impurities, in good agreement with spectroscopic results.[9]

At higher voltages beyond the ohmic regime, the current increases more strongly than linearly with increasing voltage. It is in this regime where charge-carrier multiplication by impurity impact ionization due to hot electrons sets in. Increasing the voltage further, the lower curve in Fig. 2 eventually reaches the threshold voltage V_{th} (about 0.58 V), where the nonequilibrium system of charge carriers becomes unstable and avalanche breakdown occurs. Here, for voltage bias, the current increases abruptly by several orders of magnitude, and one observes hysteresis. For current bias, one finds an S-shaped I-V characteristic with a regime of negative differential conductance (SNDC). As has been shown by LTSEM for p-type Ge (Refs. 1, 4, and 5) and n-type GaAs (Ref. 6), avalanche breakdown and the SNDC regime are accompanied by current filamentation. Further, in this regime of the I-V characteristic spontaneous resistance oscillations can be observed.[10,11]

The regime of the I-V characteristic beyond avalanche breakdown is referred to as the post-breakdown regime. Here spontaneous oscillations can also be observed, and additional branches of SNDC due to the nucleation of additional current filaments can often be seen. In the following, we concentrate on the breakdown regime and do not discuss the post-breakdown regime any further.

Turning to the upper curve in Fig. 2 taken at 8.44 K, we note that the avalanche-breakdown regime appears to be completely absent. Hence, we conclude already from Fig. 2 that there exists a strong qualitative change between the I-V characteristics for the two temperatures shown.

A typical series of I-V characteristics obtained for current-biased operation in the temperature range 4.17–6.68 K is presented in Fig. 3 with high current resolution for a restricted voltage range. On the low-temperature side the S shape due to the nucleation of a current filament can be seen. Towards higher temperatures the S shape vanishes, and the I-V characteristics change into monotonically increasing curves.

Additional insight into the breakdown behavior and the underlying physics of the I-V characteristics is obtained from time-resolved measurements. Figure 4 shows the I-V characteristic of sample 2 at 4.2 K obtained for current bias with $R_L = 10$ kΩ. The dashed-dotted and

the solid lines represent the time-averaged curves plotted with an x-y recorder. However, in addition, spontaneous oscillations of the sample voltage can be detected with an oscilloscope in the SNDC regime for current-biased operation (with $R_L = 10$ kΩ or larger). The inset shows these voltage oscillations for the points a, b, and c marked on the recorded time-averaged I-V characteristic. At low current values, these oscillations display a characteristic periodic sawtooth behavior. Apparently, these voltage oscillations are switching oscillations caused by the temporary formation of unstable current filaments in conjunction with the relaxation of the sample voltage. These oscillations can be understood as a special case of the oscillatory behavior of the electric transport, as will be shown elsewhere.[11] Here and in the following, we concentrate on the point that the time-averaged I-V characteristic only displays part of the SNDC behavior. In particular, the width of the SNDC regime can be considerably larger than shown by time-averaged I-V characteristics. To demonstrate this, let us discuss the mechanism of these switching oscillations in more detail. As displayed in Fig. 5, one oscillatory cycle can be understood as a sequence of four steps. Here the first step consists of the generation of a current filament, resulting in an increase of the sample current. During step two, the sample voltage decreases. The time constant of this process is determined by the effective capacitance of the electric circuitry connected to the sample (note that the internal dielectric relaxation time is much shorter and can therefore be neglected in the present case[11]). Thus, in step 2 this capacitance is discharged via the relatively high sample conductance until at a certain sample voltage V_h the current filament becomes annihilated, and the sample switches to the low-conductance prebreakdown state (step 3). Now the capacitance is recharged via the load resistor, and the sample voltage is increased (step 4) until at the breakdown voltage V_{th} the cycle starts again with the temporary formation of a current filament. The

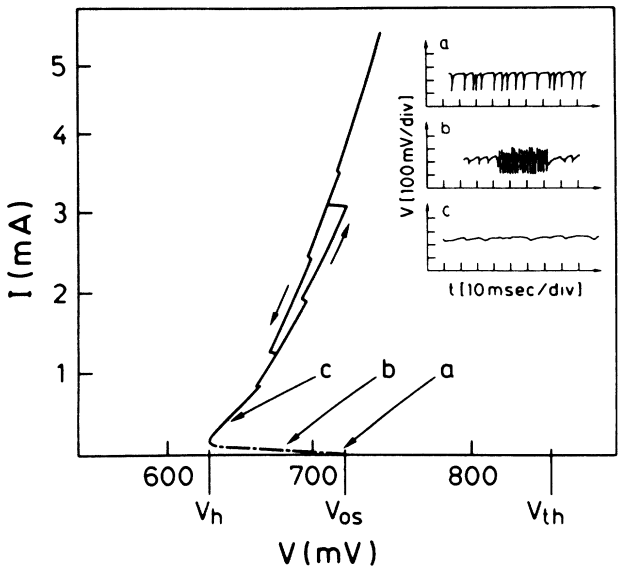

FIG. 4. Time-averaged recording of current vs sample voltage (dashed-dotted and solid lines) for sample 2 at 4.2 K ($R_L = 10$ kΩ). The inset shows time-resolved measurements of the spontaneous oscillations of the sample voltage for the operating points marked a, b, and c, respectively, on the time-averaged curve. The points marked V_h and V_{th} on the voltage axis indicate the turning points of the spontaneous voltage oscillations obtained from time-resolved measurements. V_{os} gives the time-averaged voltage where the spontaneous oscillations set in and, simultaneously, indicates the right-hand turning point of the time-averaged characteristic.

sample voltage, measured as a function of time, is the projection of the phase portrait displayed in Fig. 5(a) on the voltage axis, as seen in Fig. 5(b). Thus, this time signal contains mainly the two relaxation processes (steps 2 and 4). Clearly, this oscillatory behavior is strongly

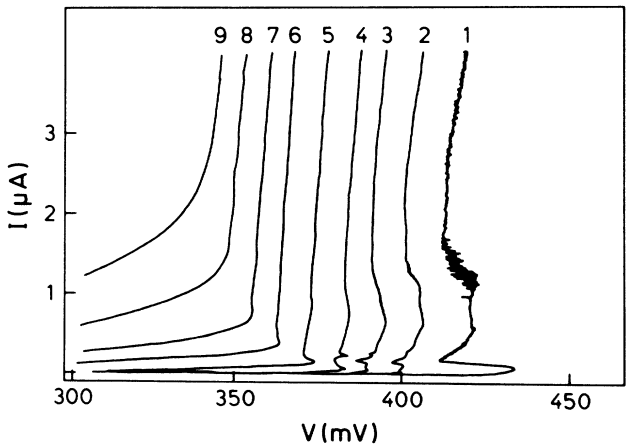

FIG. 3. Current plotted in high resolution vs the sample voltage for the following temperatures: (1) $T = 4.17$ K, (2) $T = 4.60$ K, (3) $T = 5.12$ K, (4) $T = 5.33$ K, (5) $T = 5.62$ K, (6) $T = 5.90$ K, (7) $T = 6.19$ K, (8) $T = 6.48$ K, (9) $T = 6.68$ K. Sample 1.

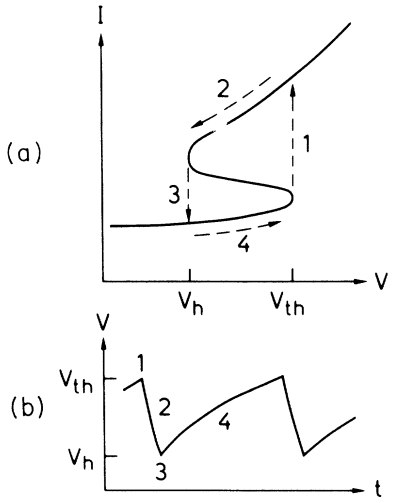

FIG. 5. Schematics of the cycle of the switching oscillations. (a) Phase portrait of the current vs the voltage showing a sequence of four steps. (b) Time dependence of the sample voltage.

affected by the electric circuitry. However, it is induced by the bistability, resulting from the electric transport properties of the bulk semiconductor material.

In fact, if a system displaying SNDC is driven into the unstable range by current control, there remain two possibilities for establishing this current: either as the spatial average (current filaments) or as the temporal average (spontaneous oscillations). The occurrence of such type of oscillations is a reliable indication for the existence of two different conducting phases in the semiconductor under the given physical conditions. Moreover, measuring for the turning points V_{th} and V_h about 850 and 630 mV, respectively (see Fig. 4), we note that during one period of this oscillation the bistable range is much larger than the SNDC regime, given by the time-averaged I-V characteristic. For instance, the right-hand turning point of the time-averaged I-V characteristic (denoted by V_{os} in Fig. 4) coincides with the onset of the switching oscillations, and the subsequent increase of the time-averaged current is a pure result of the charge transport provided by the oscillatory cycle, as discussed above. We see that the time-averaged measurements result in an essential loss of information, whereas the evaluation of the time series in the case of switching oscillations directly yields the bistable voltage range $\Delta V = V_{th} - V_h$. The actual values of V_{th} and V_h were found to vary slightly from one oscillatory cycle to another in the range of about 10% of ΔV. Due to the typical frequency range of some kHz, sufficient data for adequate averaging procedures could be accumulated in a relatively short time. The results obtained in this way are independent from the applied bias voltage V_0, as well as from the oscillatory frequency within the error limit of a few percent.[11]

Concluding this section, we emphasize that the SNDC regime associated with the current filamentation process can be quantified by means of the voltage difference $\Delta V = V_{th} - V_h$ obtained from the time-resolved measurements. In Sec. IV we investigate the variation of ΔV with increasing temperature, looking for universal scaling behavior.

IV. SCALING BEHAVIOR OF THE INSTABILITY REGIME FOR INCREASING TEMPERATURE

The experimental results presented in Sec. III indicate that with increasing temperature the S shape of the I-V characteristic vanishes, and monotonic behavior of the I-V characteristic sets in at a distinct temperature T_c. Such behavior is often classified as cusp catastrophe. Motivated by the Landau theory of equilibrium phase transitions, we describe this behavior by a third-order polynomial expansion of the voltage as a function of the current near the point (V_0, I_0),

$$V = V_0 + a(I - I_0) + b(I - I_0)^3 \tag{1}$$

setting

$$a = a_0(T - T_c), \quad a_0 > 0, \quad b > 0 . \tag{2}$$

The polynomial (1) can be obtained by minimization from the Landau functional with the conventional ansatz

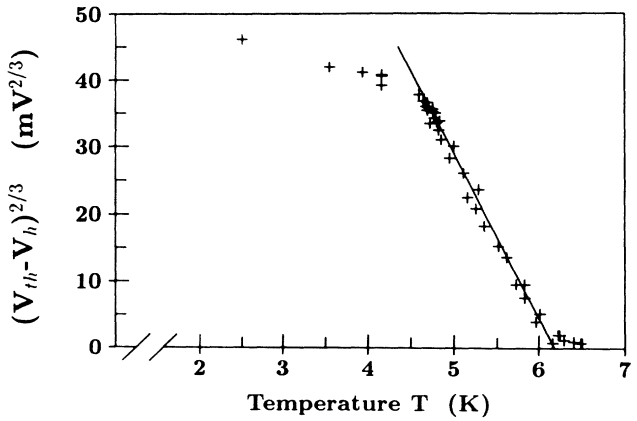

FIG. 6. $(V_{th} - V_h)^{2/3}$ obtained from the time-resolved measurements plotted vs temperature. Sample 2.

$$G(a, I, V) = (a/2)(I - I_c)^2 + (b/4)(I - I_c)^4 - I(V - V_c) ,$$

where $I - I_c$ and $V - V_c$ are interpreted as the order parameter and the ordering field, respectively, and T_c is identified as the critical temperature.

For $T < T_c$ the I-V characteristic is S shaped, and we have hysteresis. The S shape disappears at $T = T_c$. For the distance between the extremal points, one finds from (1) and (2)

$$\Delta V = V_{th} - V_h \sim (T_c - T)^{3/2} \tag{3}$$

and

$$\Delta I = I_h - I_{th} \sim (T_c - T)^{1/2} . \tag{4}$$

Using the switching oscillations as an indicator of the bistability, as discussed above, we are able to quantify the size of this bistable region in terms of their voltage amplitude $\Delta V = V_{th} - V_h$. In Fig. 6 we have plotted $(V_{th} - V_h)^{2/3}$ obtained from the time-resolved measurements versus temperature. We see that in the temperature range between 4.5 and 6.2 K the experimental data

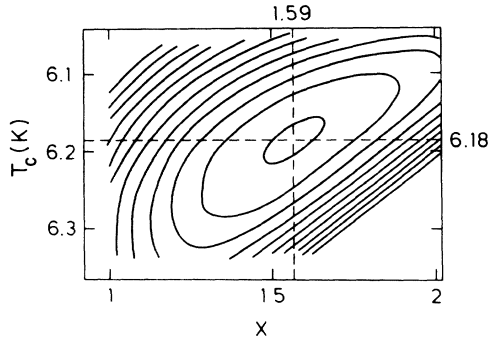

FIG. 7. Least-squares analysis for obtaining the quantities x and T_c of the proportionality $\Delta V = V_{th} - V_h \sim (T_c - T)^x$. Sample 2. The concentric contours represent successive standard deviations.

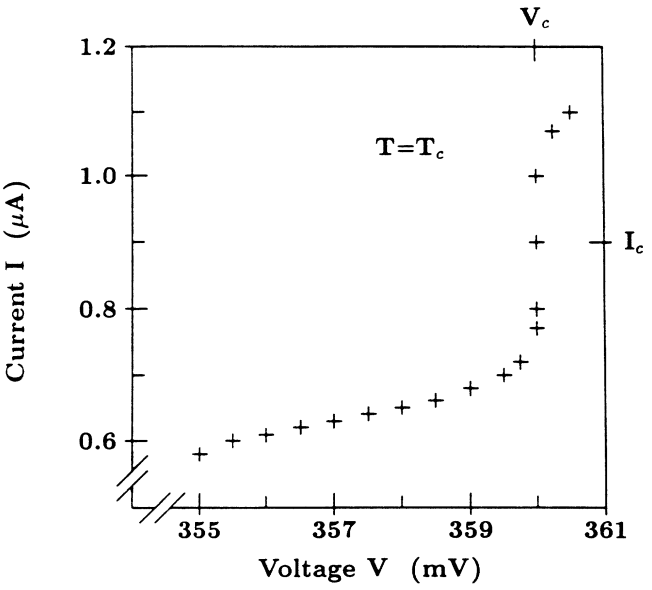

FIG. 8. Current vs voltage at $T=T_c=6.18$ K. Sample 1.

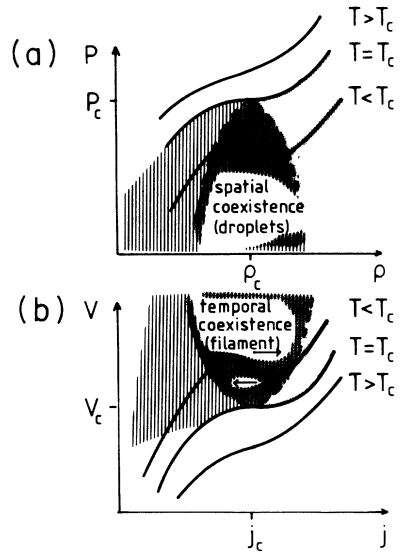

FIG. 9. Analogy between the van der Waals gas and the nonlinear electronic transport of a semiconductor. (a) Pressure p vs density ρ of the van der Waals gas for three temperatures $T<T_c$, $T=T_c$, and $T>T_c$. The spatial coexistence regime separates the homogeneous gaseous phase on the left (vertically hatched region) from the homogeneous liquid phase on the right (dotted region). (b) Voltage V vs current density j of the semiconductor for three temperatures $T<T_c$, $T=T_c$, and $T>T_c$. The temporal coexistence regime separates the low-conducting state on the left (vertically hatched region) from the high-conducting state on the right (dotted region).

agree reasonably well with the behavior expected from Eq. (3). By extrapolation of the straight line fitted to the data, we find $T_c=6.2$ K.

Of course, in a more accurate treatment both the exponent x and the temperature T_c must be subjected to a least-squares-fitting procedure, using the more general proportionality

$$\Delta V=V_{th}-V_h\sim(T_c-T)^x\ . \tag{5}$$

The results of such a least-squares analysis are shown in Fig. 7, yielding the values $T_c=6.18\pm0.07$ K and $x=1.59\pm0.10$. In Fig. 8 we present the I-V characteristic measured at $T=T_c=6.18$ K, displaying the expected inflection point in vertical direction. We note that this curve is not affected any more by temporal variations, since the voltage amplitude of the switching oscillations vanishes at $T=T_c$.

Similar to the exponent x in Eq. (5), we can now introduce the exponent y by writing at $T=T_c$

$$V-V_0\sim(I-I_0)^Y\ . \tag{6}$$

From a least-squares fit of the data of Fig. 8, we obtained $y=3.4\pm1.1$.

From our results, we conclude that the temperature dependence of the I-V characteristic displays a critical scaling behavior. It is interesting to correlate the exponents in Eqs. (4)–(6) with the critical exponents established for equilibrium second-order phase transitions.[12] For this we assume the difference of the two current densities j_1 and j_2 to be the order parameter of the phase transition. Using the conventional notation,[12] we write

$$j_1-j_2\sim(T_c-T)^\beta \tag{7}$$

and for $T=T_c$

$$V-V_c\sim(j-j_c)^\delta\ . \tag{8}$$

The Landau theory yields the following values of the critical exponents:[12] $\beta=\frac{1}{2}$, $\delta=3$. We see that the exponent x defined in Eq. (5) can be identified as $x=\beta\delta$ and the exponent y defined in Eq. (6) as $y=\delta$. Our values of x and y are, within their error limits, consistent with the Landau theory.

V. ANALOGY WITH THE VAN DER WAALS GAS

We have found that the nonlinear electric current transport in p-type Ge in the avalanche-breakdown regime shows strong similarities to the critical phenomena well known for equilibrium second-order phase transitions. Therefore, it is useful to consider this analogy in more detail. As an example for the equilibrium system, we take the van der Waals gas. In Fig. 9(a) we show schematically the pressure p plotted versus the density ρ of the van der Waals gas for three temperatures $T<T_c$, $T=T_c$, and $T>T_c$, where T_c is the critical temperature. The dashed line indicates the coexistence regime separating the homogeneous gaseous phase on the left from the homogeneous liquid phase on the right. The latter regime is characterized by the *spatial coexistence* of the two phases. The order parameter is usually defined as the difference between the density of the liquid and the gaseous phase, $\rho_{\text{liq}}-\rho_{\text{gas}}$.

Figure 9(b) shows the analogous situation for the non-

linear current transport in p-type Ge. The voltage is plotted versus current density again for three temperatures $T < T_c$, $T = T_c$, and $T > T_c$. (Note that increasing temperature now corresponds to the sequence of the curves from top to bottom.) Again the dashed line indicates the coexistence regime separating the low-conducting state on the left from the high-conducting state on the right. Here it is important to note that the van der Waals gas represents a system of equilibrium thermodynamics, which is only defined in the limit of infinite size (thermodynamic limit). In contrast, in our semiconductor system we deal with a nonequilibrium phase transition. Furthermore, we have to take into account the finite system size, i.e., the concrete sample dimension is in the order of the minimal structure size (filament diameter).[13] In concentrating on the onset of avalanche breakdown, we deal with the generation of a single current filament. In the parameter range of the switching oscillations of the current filament, the coexistence regime is now characterized by the *temporal coexistence* of two states. One corresponds to the homogeneously nonconducting phase on the left of Fig. 9(b). The other is characterized by the existence of a current filament,[11,14] representing the high-conducting phase on the right of Fig. 9(b). Clearly, the fact that a current filament can exist only above a distinct minimal cross-sectional size also plays an essential role in this temporal coexistence regime.

ACKNOWLEDGMENTS

Financial support of this work by a grant of the Deutsche Forschungsgemeinschaft is gratefully acknowledged.

[1]R. P. Huebener, K. M. Mayer, J. Parisi, J. Peinke, and B. Röhricht, Nucl. Phys. B **2**, 3 (1987).
[2]R. P. Huebener, J. Peinke, and J. Parisi, Appl. Phys. A **48**, 107 (1989).
[3]E. Schöll, *Nonequilibrium Phase Transitions in Semiconductors* (Springer-Verlag, Berlin, 1987).
[4]K. M. Mayer, R. Gross, J. Parisi, J. Peinke, and R. P. Huebener, Solid State Commun. **63**, 55 (1987).
[5]K. M. Mayer, J. Peinke, B. Röhricht, J. Parisi, and R. P. Huebener, Phys. Scr. **T19**, 505 (1987).
[6]K. M. Mayer, J. Parisi, and R. P. Huebener, Z. Phys. B **71**, 171 (1988).
[7]B. Röhricht, R. P. Huebener, J. Parisi, and M. Weise, Phys. Rev. Lett. **61**, 2600 (1988).
[8]M. Lehr, Thesis, University of Tübingen, 1989 (unpublished).
[9]T. C. Harman and I. Melngailis, Appl. Solid State Sci. **4**, 136 (1974).
[10]J. Peinke, A. Mühlbach, R. P. Huebener, and J. Parisi, Phys. Lett. **108A**, 407 (1985).
[11]U. Rau, W. Clauss, A. Kittel, M. Lehr, M. Bayerbach, J. Parisi, J. Peinke, and R. P. Huebener, Phys. Rev. B (to be published).
[12]L. D. Landau and E. M. Lifschitz, *Statistische Physik I* (Akademie Verlag, Berlin, 1987), p. 457.
[13]K. M. Mayer, R. P. Huebener, and U. Rau, J. Appl. Phys. **67**, 1412 (1990).
[14]U. Rau, K. M. Mayer, J. Parisi, J. Peinke, W. Clauss, and R. P. Huebener, Solid State Electron. **32**, 1365 (1989).

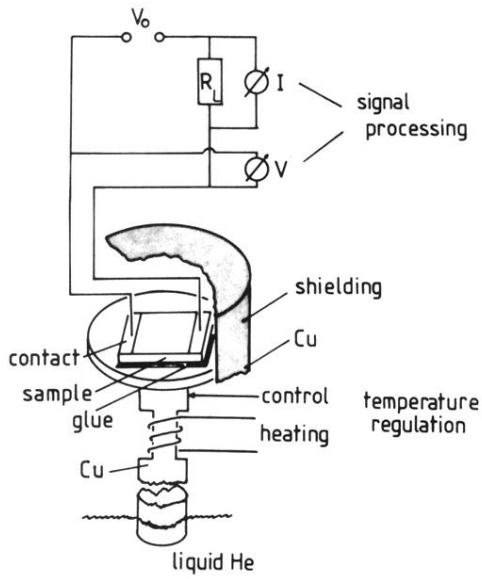

FIG. 1. Schematics of the sample configuration and the electronic measuring circuit.

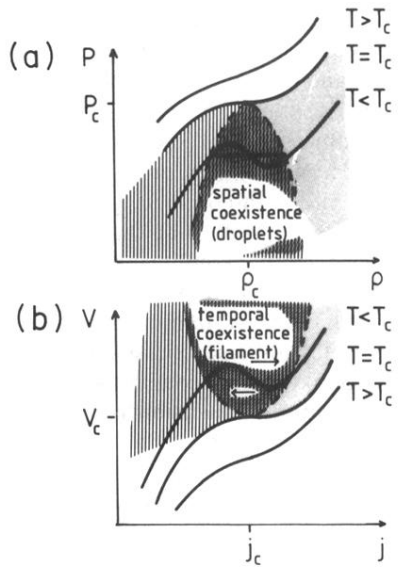

FIG. 9. Analogy between the van der Waals gas and the nonlinear electronic transport of a semiconductor. (a) Pressure p vs density ρ of the van der Waals gas for three temperatures $T < T_c$, $T = T_c$, and $T > T_c$. The spatial coexistence regime separates the homogeneous gaseous phase on the left (vertically hatched region) from the homogeneous liquid phase on the right (dotted region). (b) Voltage V vs current density j of the semiconductor for three temperatures $T < T_c$, $T = T_c$, and $T > T_c$. The temporal coexistence regime separates the low-conducting state on the left (vertically hatched region) from the high-conducting state on the right (dotted region).